IUST
Iran University of Science and Technology

Iranian Journal of Electrical and Electronic Engineering

Journal Homepage: ijeee.iust.ac.ir

Research Paper

Design and Implementation of a High-Precision Position Controller for Permanent Magnet Synchronous Motor Based on a New Gain Scheduling Approach

S. H. Montazeri*, A. Damaki Aliabad*(C.A.), F. Zareh*, and S. Aghaei*

Abstract: The direct drive permanent magnet synchronous motor (DD-PMSM) is a suitable choice for high-precision position control applications. Among various control methods of this motor, the vector control approaches especially the field oriented control has a high-performance in the industrial drives. In this method, the components of stator current are controlled independently and as a result, the torque and flux are controlled continuously. Since there are some limitations and constraints in the motor, inverter, and control system, a new anti-windup gain scheduling PID controller based on the adaptive control principles is proposed for the position control loop. In the proposed method, different values are assigned to coefficients of the PID controller according to the position error to achieve high precision. Also, a very high-accuracy encoder and an ARM processor are used for measuring the instantaneous position and implementation of the proposed method, respectively. The simulation and experimental results validate the effectiveness, high accuracy, and good dynamic behavior of the proposed control method.

Keywords: Anti-Windup Gain Scheduling Method, Field-Oriented Control, High-Precision Control, Permanent Magnet Synchronous Motor.

1 Introduction

PERMANENT magnet synchronous motor (PMSM) is used widely in industrial and automotive applications. This is due to their significant characteristics such as high controllability, high efficiency, high torque-to-inertia ratio, high torque and power density, low torque ripple, good dynamic performance, robustness, etc. [1-3]. On the other hand, a direct drive (DD) motor which is directly coupled with load without any mechanical components offers significant advantages over its indirect counterparts including eliminating the backlash, reducing the friction, simplifying the mechanical structure, etc. [4, 5]. Since a direct drive motor has multiple poles, it is capable to produce the desired torque within the full speed region [6]. As a result, the DD-PMSM is often employed in high-performance motor drives.

Generally, PMSM control methods can be divided into scalar and vector control. In the scalar method, only the magnitude and frequency of voltage, current, and flux linkage vectors are controlled based on the steady-state relationships. Therefore, this method cannot control the motor characteristics during the transient period [7]. On the other hand, it has low performance at low speed and slow response to the reference changes. Thus, this method is not suitable for high-performance precise control objectives. On the other side, the vector control approach controls the magnitude, frequency, and instantaneous position of voltage, current, and flux vectors. The most popular vector control methods are field-oriented control (FOC) and direct-torque control (DTC). In the DTC, the inverter switching states are controlled directly in order to reduce the torque and flux errors within the hysteresis bands. Some disadvantages of DTC are torque and flux control difficulties at very low speed, high noise level at low speed, variable switching frequency, lack of direct

Iranian Journal of Electrical and Electronic Engineering, 2021.
Paper first received 14 May 2019, revised 28 January 2020, and accepted 31 January 2020.
* The authors are with the Electrical Engineering Department, Yazd University, Yazd, Iran.
E-mails: s.hamidmontazeri@gmail.com, alidamaki@yazd.ac.ir, farhadzare1992@yahoo.com, and aghaei@yazd.ac.ir.
Corresponding Author: A. Damaki Aliabad.
https://doi.org/10.22068/IJEEE.17.1.1502

current control, and high current and torque ripples [79]. Thus, DTC method is not suitable for precise control, too. The FOC controls the current vector components independently and for this reason, the torque and flux are controlled continuously and high-performance and precise control has been achieved. Therefore, in this paper, the FOC method is used and the three-loop control system uses PI and PID controllers for current and position control loops, respectively.

In some literatures, the fixed coefficients have been used for the position controller which they have tuned using Ziegler Nichols method [10], neural network method [11], intelligent algorithms [12], etc. Also, the combination of various tuning methods has been applied to adjust the controller including neural network based adaptive controller [13], neural network based robust controller [14], combination of fuzzy and sliding mode controller to achieve robust controller [15], adaptive fuzzy sliding mode controller [16], and adaptive fuzzy logic [17] methods. In [18], a fuzzy controller and a typical PI controller is used for the position and speed control loops, respectively.

In the FOC method, the reference current vectors are controlled in the inner feedback loops to achieve desired torque for the minimum current and fast dynamics. This reference current is generated in the outer feedback loop (the position control loop) which is limited to a maximum value due to the converter protection, the core magnetic saturation, and thermal constraints of the motor [19]. Thus, the traditional tuning methods including the conventional gain scheduling approach, can lead to saturation in the outer control loop and the integral controller increases the output signal due to over-charging of the integrator when the actuator is saturated. This inappropriate performance is referred to as “windup” phenomenon.

In this paper, due to limitations and constraints in the motor, inverter, and control system as well as in order to achieve high accuracy and a good dynamic behavior, variable coefficients based on an adaptive control method are chosen for the position controller. In the proposed method, different values are assigned to the PID controller coefficients according to the position error and regarding the different features of the control systems with saturations [19-23], an anti-windup gain scheduling PID controller is proposed and implemented.

In addition, in order to increase the accuracy of the control system, an absolute encoder with a resolution of 720×10^{12} increments per revolution has been used to measure the rotor position. On the other hand, the proposed control method is implemented on an advanced RISC machine (ARM) processor. High accuracy and processing rate and low cost are the main advantages of the ARM processors.

The remaining parts of the paper are organized as follows. Section 2 briefly introduces the FOC method and the space vector pulse width modulation (SVPWM) algorithm and describes the block diagram of the control system. Section 3 presents the proposed anti-windup gain scheduling PID method. Simulation and experimental results are shown in Sections 4 and 5, respectively. Finally, Section 6 concludes the paper.

2 Field-Oriented Control

In the FOC method, vector components of the stator current (i.e. i_d and i_q) are chosen as state variables and the stator currents is controlled in a high-bandwidth loop using a high-frequency power inverter. Thus, the current equations are eliminated and the overall order of the system decreases.

Fig. 1 shows the block diagram of the nonsalient-pole PMSM position control system in the FOC method. In the current control loops, the d and q axis currents are compared with the reference values and the voltage vector is determined using PI controllers. Then, to determine the SVPWM block input, the α-β frame

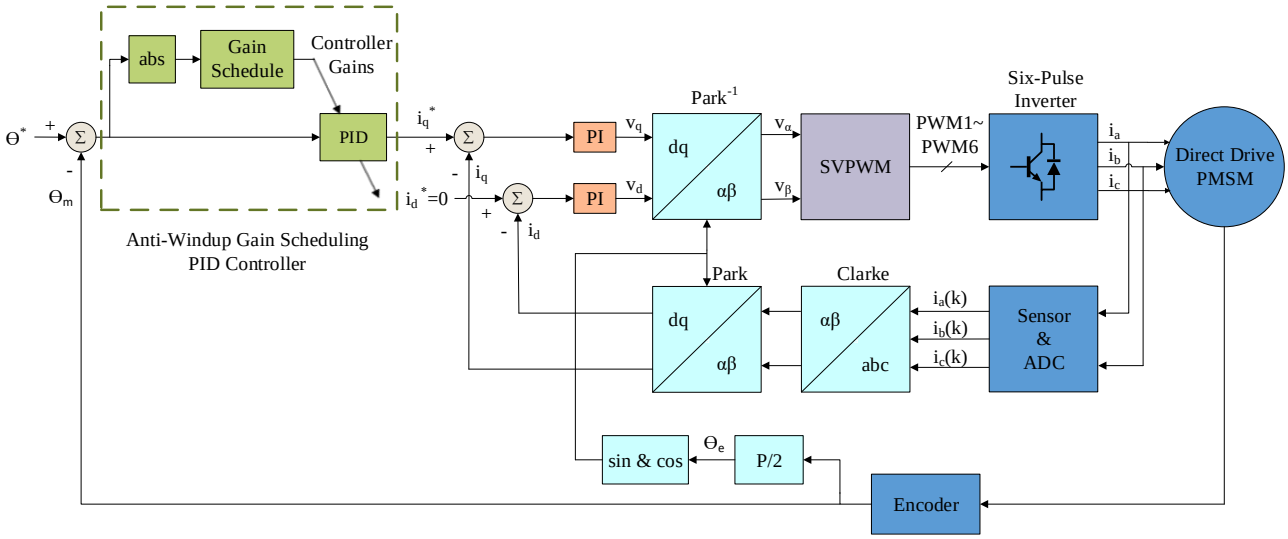

Fig. 1 The block diagram of the position control system in the FOC method.

voltages are calculated using Park^{-1} transformation. Finally, SVPWM method generates the desired switching pulses for the six-pulse inverter to direct the PMSM to the reference position.

The typical structure of three-phase six-pulse inverter is shown in Fig. 2. SVPWM method uses DC link voltage optimally and switching signals can be generated from the α-β frame voltages directly. Thus, this method can be easily implemented in the vector control.

In a three-phase inverter, the output voltage vector based on switches' commands is given as (1) using the Clarke transformation.

$$\vec{U} = \frac{2}{3} V_{DC} (S_a + a.S_b + a^2.S_c) \quad (1)$$

where $\vec{U}$ represents the inverter voltage vector in α-β frame and V_{DC} indicates the DC-link voltage. The constant value of "a" is equal to $1\angle 120°$ and S_a, S_b, and S_c are equal to "1" or "0" when corresponding switches are "on" or "off", respectively. Thus, there are eight possible combinations according to the on/off state of upper switches, which are called basic space vectors. The basic vectors, corresponding switching states and the output voltage are listed in Table 1 and Fig. 3 shows the basic vector space.

Although the six-pulse inverter can only generate six discrete non-zero voltage vectors, but by combination of the adjacent vectors and the zero vector as (2), it is possible to generate each voltage vector with desired amplitude and phase angle:

$$\vec{U} = \frac{T_1}{T} U_{60\times(n-1)} + \frac{T_2}{T} U_{60\times n} + \frac{T_0}{T} (O_0 \text{ or } O_7) \quad (2)$$

where n is the sector number, T is equal to half of the carrier wave period and T_0, T_1, and T_2 are the operation time of zero and adjacent voltage vectors, respectively.

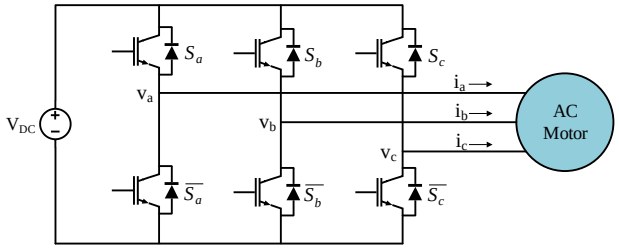

Fig. 2 The structure of three-phase inverter and motor.

Table 1 Switching states and basic vectors.

Vector	S_a	S_b	S_c	$\vec{U}$	U_α	U_β
O_0	0	0	0	0	0	0
U_{240}	0	0	1	$2/3V_{DC}\angle 240°$	$-V_{DC}/3$	$-V_{DC}/\sqrt{3}$
U_{120}	0	1	0	$2/3V_{DC}\angle 120°$	$-V_{DC}/3$	$V_{DC}/\sqrt{3}$
U_{180}	0	1	1	$2/3V_{DC}\angle 180°$	$-2/3V_{DC}$	0
U_0	1	0	0	$2/3V_{DC}\angle 0°$	$2/3V_{DC}$	0
U_{300}	1	0	1	$2/3V_{DC}\angle 300°$	$V_{DC}/3$	$-V_{DC}/\sqrt{3}$
U_{60}	1	1	0	$2/3V_{DC}\angle 60°$	$V_{DC}/3$	$V_{DC}/\sqrt{3}$
O_7	1	1	1	0	0	0

To compare the reference with the measured current, the three-phase stator currents and instantaneous rotor position are measured and α-β and d-q frame currents are calculated using Clarke and Park transformations, respectively. Since, the sum of three-phase stator currents is equal to zero, two-phase sampling is sufficient. On the other hand, the electromagnetic torque in a non-salient pole PMSM is calculated as:

$$T_{el} = \frac{3P}{4} \Psi_{PM} i_q = K_i i_q \quad (3)$$

where P is the number of poles and Ψ_{PM} decades the permanent magnet flux linkage. As seen, the torque value is proportional to i_q and i_d does not affect the torque and only increases the stator flux. For this reason, to produce the maximum torque-to-current ratio, the i_d current should be equal to zero and the torque is controlled with i_q. Therefore, the d-axis will be decoupled from the q-axis.

However, the q-axis is coupled to the d-axis by the q-axis flux. Often, this coupling can be considered as a low-frequency disturbance that is eliminated by the d-axis controller. On the other way, similar to the DC motor, the back-EMF voltage disturbs in the current control loop that this disturbance is compensated by PI controllers in the steady-state.

The q-axis reference current is determined by comparing the measured rotor position with the reference value and using a PID controller in the outer control loop. Then, it is applied to the current control loop to produce the required torque.

The transformation between stationary a-b-c frame, stationary α-β frame and synchronous d-q frame are described as following [18] where f denotes voltage or current:

- Clarke: stationary a-b-c frame to stationary α-β frame

$$\begin{bmatrix} f_\alpha \\ f_\beta \end{bmatrix} = \begin{bmatrix} \frac{2}{3} & -\frac{1}{3} & -\frac{1}{3} \\ 0 & \frac{1}{\sqrt{3}} & -\frac{1}{\sqrt{3}} \end{bmatrix} \begin{bmatrix} f_a \\ f_b \\ f_c \end{bmatrix} \quad (4)$$

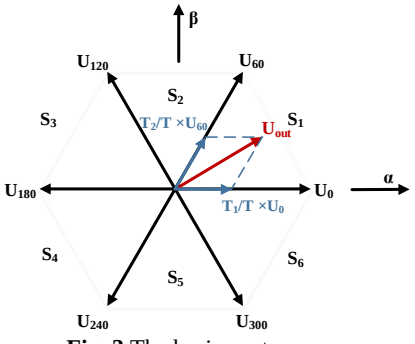

Fig. 3 The basic vector space.

- Clarke^{-1}: stationary α-β frame to stationary a-b-c frame

$$\begin{bmatrix} f_a \\ f_b \\ f_c \end{bmatrix} = \begin{bmatrix} 1 & 0 \\ -\frac{1}{2} & \frac{\sqrt{3}}{2} \\ -\frac{1}{2} & -\frac{\sqrt{3}}{2} \end{bmatrix} \begin{bmatrix} f_\alpha \\ f_\beta \end{bmatrix} \quad (5)$$

- Park: stationary α-β frame to rotating d-q frame

$$\begin{bmatrix} f_d \\ f_q \end{bmatrix} = \begin{bmatrix} \cos\theta_e & \sin\theta_e \\ -\sin\theta_e & \cos\theta_e \end{bmatrix} \begin{bmatrix} f_\alpha \\ f_\beta \end{bmatrix} \quad (6)$$

- Park^{-1}: rotating d-q frame to stationary α-β frame

$$\begin{bmatrix} f_\alpha \\ f_\beta \end{bmatrix} = \begin{bmatrix} \cos\theta_e & -\sin\theta_e \\ \sin\theta_e & \cos\theta_e \end{bmatrix} \begin{bmatrix} f_d \\ f_q \end{bmatrix} \quad (7)$$

where θ_e is the electrical position of the motor and is calculated in terms of the number of poles (P) and the mechanical position (θ_m) as (8).

$$\theta_e = \frac{P}{2}\theta_m \quad (8)$$

3 The Proposed Tuning Method for Position Controller Coefficients

In a PID controller, the control signal $u(t)$ can be expressed mathematically as:

$$u(t) = K_p e(t) + K_i \int_0^t e(\tau)d\tau + K_d \frac{de(t)}{dt} \quad (9)$$

where K_p, K_i, and K_d, all non-negative, denote the proportional (P), integral (I), and derivative (D) coefficients, respectively. Regarding the effects of these terms, the PID controller coefficients should be tuned to reduce the rise and settling time, to prevent the overshoot, and to eliminate the tracking error. Generally, the following three starting points are useful:

- K_p is able to decrease the rise time.
- K_d is able to reduce overshoot and settling time.
- K_i is able to eliminate the steady-state error in step response.

Table 2 illustrates the effects of independently increasing of K_p, K_i, and K_d on characteristics of the closed-loop step response.

Table 2 Effects of independent increasing of Kp, Ki, and Kd parameters on the closed-loop step response [22].

Parameter	K_p	K_i	K_d
Rise time	Decrease	Decrease	Minor change
Overshoot	Increase	Increase	Decrease
Settling time	Small increase	Increase	Decrease
Steady-state error	Decrease	Eliminate	No effect in theory
Stability	Degrade	Degrade	Improve

Traditionally, the PID controller is widely adopted to control the PMSM in industrial applications owing to its simplicity, clear functionality, and effectiveness. However, a big problem of the conventional PID controller is its sensitivity to the system uncertainties. Thus, the control performance can be seriously degraded under parameter variations [22]. On the other hand, the adjusted parameters cannot work optimally for various operating conditions such as starting up, near the target point, etc. This will be more serious when the controlled system and actuator are subjected to some constraints.

In this paper, to overcome this problem and to reach high precise control, a new gain scheduling method by considering the constraints is proposed for coefficients of the position controller which is different from the typical gain scheduling tuning method. The tuning principles of the gain schedule in the typical method is as follows which are described for the step-response diagram as shown in Fig. 4:

1) When the value of tracking error is large (for example, at point "A"), a large control signal should be applied to the system in order to reach a fast rise time. For this purpose, a big proportional and integral and small derivative gains are needed.
2) When the system closes to the reference point (point "B" in Fig. 5), a small control signal should be applied to the system to prevent the system overshoot. Therefore, the coefficient of the derivative controller should be increased and the proportional and the integral controllers should be decreased.

The impact of limitations on tuning the position controller and the proposed anti-windup gain scheduling method are presented in the following.

3.1 Impacts of Constraints on Tuning of Position Controller Coefficients

In PMSMs, below base speed, the maximum torque is limited by the maximum allowed current of the inverter according to the power switch rating and the motor based on its thermal (i.e. reliability) constraints. In this

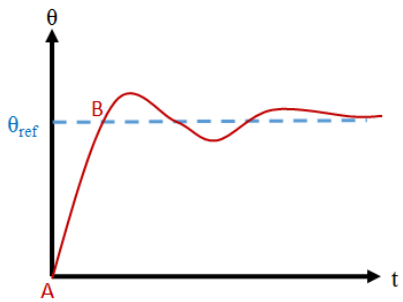

Fig. 4 The typical step-response diagram.

operating region, maximum torque per ampere control is applied. Above base speed, the inverter supplies the motor with the maximum voltage depending on the DC-link voltage and modulation strategy.

If an actuator that realizes the control action has a hard constraint or saturation limitation on its range of response to the control signal produced by an integrator, it causes the phenomenon of "windup". The presence of the integrator along with the inevitable saturation on the control signal leads to an increase in the output signal due to over-charging of the integrator when the actuator is saturated. This causes low-frequency oscillations, excess overshooting amplitude, and large settling time and may lead to instability. Generally, a usual way to tackle this effect called "anti-windup" strategy [18-20] leads the integrator to begin off until the response falls back into under saturated range.

The windup phenomenon will be intensified when the integrator coefficient is very large. In this project, to reach high precision control, large proportional and integrator coefficients are needed to excite the actuator when the smallest error is appeared in the motor position. Both of these coefficients lead to a large overshoot and may lead to instability. Due to the voltage and current constraints of the inverter as well as the inherent limitations of the control system, the conventional gain scheduling methods are not suitable here. Therefore, to overcome the wind-up and to reach high precision control performance, a recovered gain scheduling method is proposed which is named here "anti-windup gain scheduling PID method".

3.2 The Proposed Anti-Windup Gain Scheduling Method

As mentioned above, the aim of this paper is to achieve high precise position control of PMSM with a good dynamic behavior from start-up to the target point. Two problems, which may be arisen during the control of PMSM, are the nonlinearity and uncertainty in parameters and saturation of the system. Thus, because of the mentioned limitations, the conventional gain scheduling method for tuning coefficients of the PID controller does not create a satisfactory behavior for the control system. In order to tackle these limitations, the "anti-windup gain scheduling PID controller" is proposed in this section. The distinguished features of the proposed method are the change of controller coefficients by changing the system conditions, lack of estimation, and simplicity of implementation.

According to Fig. 4, the adjusting algorithm of anti-windup gain scheduling PID is proposed as follows:

1) At point "A", large values for K_p and K_i will saturate the system due to the voltage and current limitations. Thus, medium coefficients are chosen for large errors.
2) When the error becomes small (such as the point "B"), because the control signal is week, the reference current does not produce enough torque and the motor may not reach the reference position with a good dynamic behavior. Since very high accuracy is required, it is not suitable to decrease K_p and K_i coefficients in small errors. Therefore, when the motor reaches point "B", these coefficients not only are not reduced, but also they are increased. In addition, to prevent windup, the integrator memory becomes zero before reaching this point. Also, K_d is increased to brake the motor to prevent the overshoot (regarding to the large proportional gain), and to minimize the settling time.
3) In the interval between points "A" and "B", the coefficients are changed in several stages from primary values to be achieved a soft behavior.

4 Simulation

To verify the proposed control method, a 14-pole three-phase DD-PMSM is simulated and the limitations and constraints of the motor and control system are considered. The motor and load specifications are listed in Table 3. In this motor, the air gap flux and the back-EMF voltage are sinusoidal and the cogging torque and the torque ripple are very low. The limitations considered for the control system are the voltage and current. The DC-link voltage and the stator currents are limited to 300 V and 10.5 A, respectively.

In this section, the PID controller coefficients are tuned for three cases including fixed coefficients, based on the conventional gain scheduling method, and based on the proposed method. For the state of fixed coefficients, three series of gains (small, medium, and large) are considered and for the conventional and proposed gain scheduling method, the PID controller is tuned for two and six intervals of the position error, respectively. The coefficients related to these three cases are listed in Tables 4 to 7.

Table 3 The PMSM and load data.

Quantity	Symbol	Value
Phase number	-	3
Pole number	P	14
Nominal frequency	f	35 Hz
Rated torque	T_n	45 N.m
Rated speed	n_m	250 rpm
Rated current	I_s	3.5 A
Maximum current	I_{max}	10.5 A
Rotor inertia	J	0.065 kg.m^2
Back-EMF THD	THD_{EMF}	0.58 %
Back-EMF constant	-	1.08 V/rpm
Cogging torque	-	0.24 N.m
DC-link voltage	V_{DC}	300 V
Switching frequency	f_s	20 kHz
Load torque	T_L	5 N.m
Load inertia	J_L	1 kg.m^2

Table 4 The coefficients of fixed PID controllers.

PID controllers	K_p	K_i	K_d
PID 1	5	0.1	0.07
PID 2	8	4	0.16
PID 3	15	10	0.2

Table 5 PID controller coefficients for each position error in the conventional gain scheduling method.

Error intervals	K_p	K_i	K_d
Err > 1	10	6	0.2
Err < 1	6	4	0.3

Table 6 PID controller coefficients for each position error in the anti-windup gain scheduling method.

Error intervals	K_p	K_i	K_d
Err > 100	5	0.1	0.07
10 < Err < 100	5	0.1	0.11
1 < Err < 10	6	0.5	0.127
0.1 < Err < 1	8	4	0.16
0.01 < Err < 0.1	10	8	0.2
Err < 0.01	15	10	0.2

Table 7 PI controller coefficients of the current loops.

Current loop controllers	K_p	K_i
PI (d-axis current)	3	0.5
PI (q-axis current)	15	0.1

As listed in these Tables, according to section 4, in the conventional gain scheduling method, large proportional and integral coefficients are considered for large errors (e.g. more than 1 degree) and when the position error becomes small, the proportional and integral coefficients are decreased and the derivative coefficient is increased. However, in the proposed method, the large proportional and integral coefficients are not necessary for large errors (e.g. an error of more than 100 degrees) and a large derivative gain slows down the system. Hence, in the proposed anti-windup gain scheduling method, the coefficients are chosen less than those in smaller errors. On the other hand, when the rotor position approaches the reference value and the error signal becomes small, the integral, proportional, and derivative coefficients are increased.

The PI controllers related to current control loops have no much effect on the position control. Thus, fixed coefficients are determined for them listed in Table 10.

For the simulation, a square pulse of 0 to 25 degrees with a period of 0.3 seconds is considered as the reference position. Figs. 5(a), 5(b), and 5(c) show the reference and motor position with fixed PID controller, conventional and anti-windup gain scheduling PID controllers, respectively. As seen, in the fixed PID for various cases and the conventional gain scheduling method, the output has overshoot, long settling time and steady-state error due to system constraints. However, in the proposed method, the motor follows the input changes in a short rise time and without overshoot.

The mechanical speed of rotor is shown in Fig. 6. As illustrated, when the error of position is large, the speed

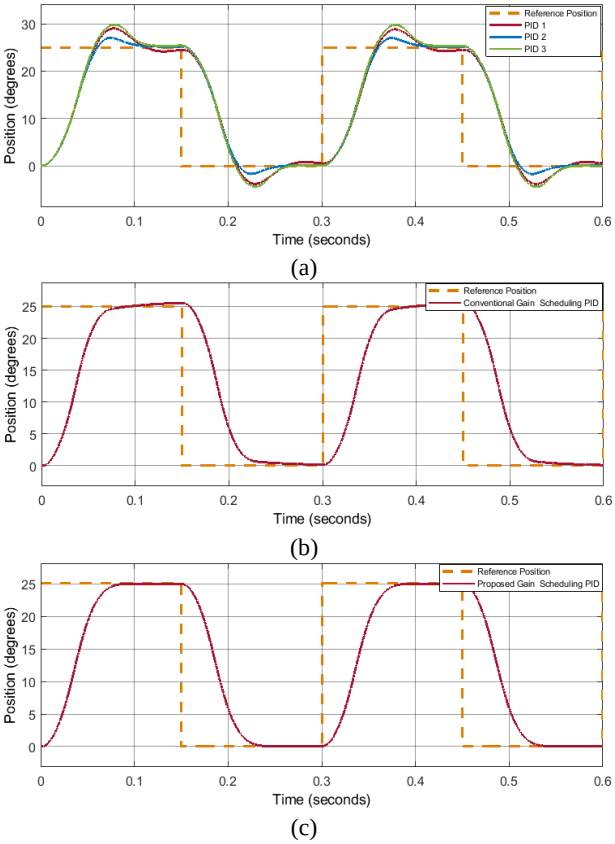

Fig. 5 The simulated waveforms for the pulse input with a) fixed PID controllers, b) conventional gain scheduling PID, and c) anti-windup gain scheduling PID controller.

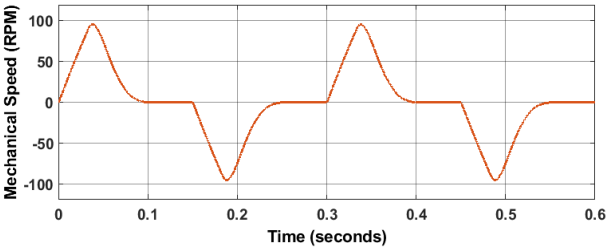

Fig. 6 Motor mechanical speed for the pulse input.

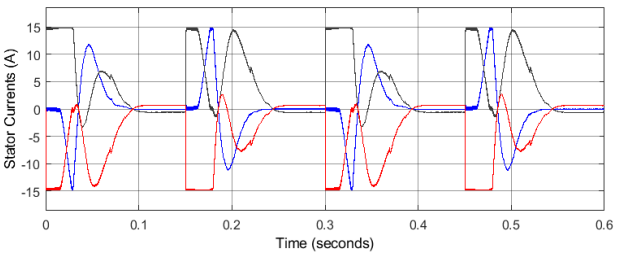

Fig. 7 The three-phase stator currents.

of motor is increased and when the motor reaches the reference input, it becomes zero. Fig. 7 illustrates the three-phase stator currents when the proposed control method is applied.

The currents of d-q frame have been shown in Fig. 8. As expected, the flux producing current is set to zero and the torque producing current changes according to the position error.

5 Implementation of the Proposed System

The test setup including DD-PMSM and the position control system are shown in Fig. 9. Since the proposed control has huge computations and high accuracy is expected, a 32 bits Cortex-M3 ARM processor is used to implement the control system. High processing speed, low noise sensitivity in industrial environments, and low cost are the main advantages of this processor. Also, in order to achieve high precision, an extremely accurate encoder is used to measure the rotor position. This absolute type encoder has a resolution of 720×10^{12} per revolution and follows the synchronous serial interface (SSI) standard.

In the following, at first, the controller coefficients are tuned and then the experimental results of the position control system are presented.

5.1 Tuning the Coefficients of Controllers

The controller coefficients should be tuned again because the test is done under the no-load condition. Moreover, in practice, the delays in the controller and the inverter, noise, motor static friction, and mechanical errors change the system condition and for this reason, the coefficients calculated in section 5 are not effective and should be re-tuned. Hence, according to the aforementioned tuning method and using the try and error method, the coefficients are determined and listed in Tables 8 and 9. For this purpose, various errors with different amplitudes are applied to the system and then the suitable coefficients are chosen for each error intervals by investigation of the system performance. The PID controller coefficients are determined for six intervals of the position error and fixed coefficients are chosen for the current controllers.

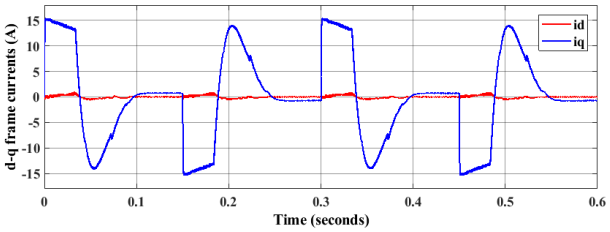

Fig. 8 d-q frame currents.

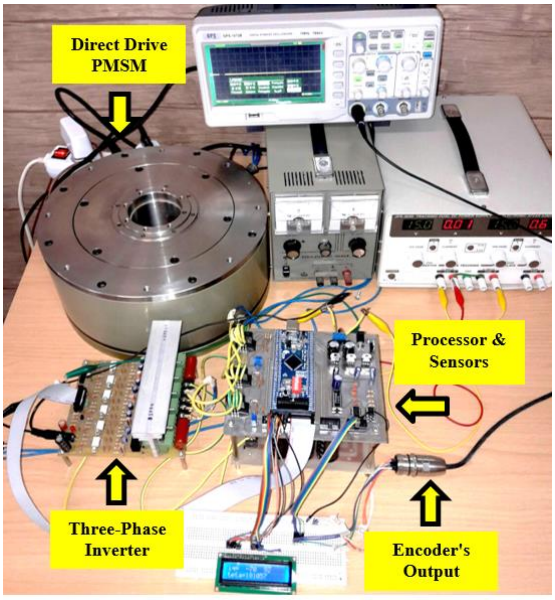

Fig. 9 The experimental set-up.

5.2 Experimental Results

The experimental results of the position control system under the no-load condition are presented in this section. In the first test, the reference values of 30 and 200 degrees are applied to the control system. The final position of the motor and the steady-state values of i_d and i_q are presented in Table 10. Also, the position variation of the motor for the reference value of 200 degrees is shown in Fig. 10. As the results show, the accuracy of the proposed control system is less than 0.001 degrees.

In the second test, the step-response of the system when the reference angle is changed from zero to 200 degrees is shown in Fig. 11. As seen, the motor follows the reference position and no instability, overshoot, and steady-state error is observed in the motor position.

Finally, a ramp reference input with the value of 5 degrees per second is applied to the system and the

Table 8 PID controller coefficients for each position error.

Error intervals	K_p	K_i	K_d
Err > 100	5	0.1	0.1
10 < Err < 100	5	0.1	0.1
1 < Err < 10	6	0.5	0.1
0.1 < Err < 1	8	4	0.2
0.01 < Err < 0.1	10	8	0.3
Err < 0.01	15	10	0.3

Table 9 PI controller coefficients of the current loops.

Current loop controllers	K_p	K_i
PI (d-axis current)	3	0.5
PI (q-axis current)	2	0.1

Table 10 Experimental results for the fixed position input.

Reference position	Motor position	I_d [A]	I_q [A]
30 degrees	30 ± 0.001 degrees	0.001	0.003
200 degrees	200 ± 0.001 degrees	0.001	0.002

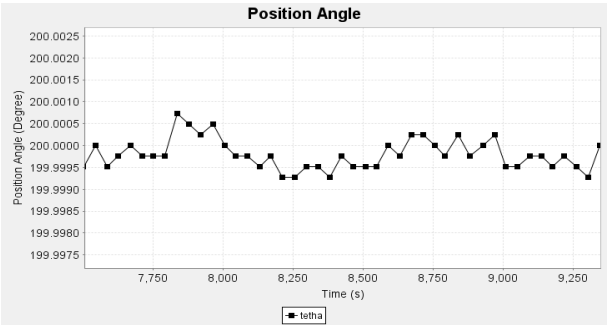

Fig. 10 The rotor position for the reference input of 200 degrees in the steady-state.

position variation of the motor is illustrated in Fig. 12. In this case, the error between the reference and measured position is illustrated in Fig. 13. As seen from these figures, after a short transient period (0.4 second), the motor follows the ramp position and the error becomes very small (less than 0.05 degree).

6 Conclusion

In this paper, a high-precision position control system for a DD-PMSM has been proposed. The FOC method has been used to control the motor and the switching pulses for six-pulse inverter has been generated based on the SVPWM algorithm. Regarding the different features of control systems with saturation, an anti-windup gain scheduling PID controller has been designed and implemented for the position control loop. The experimental results have shown that the proposed system has a precision less than 0.001 degrees and the rotor position follows the reference input in a short time without any overshoot, instability, and steady-state error. The main advantages of the proposed method are the fast changes of controller coefficients by changing the system conditions, lack of estimation, high accuracy,good dynamic behavior of the control system, and simplicity of the implementation.

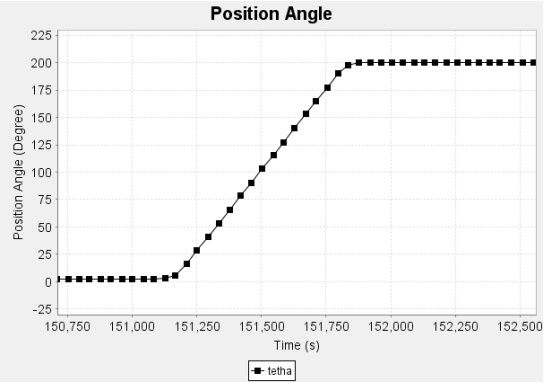

Fig. 11 The step-response of the control system.

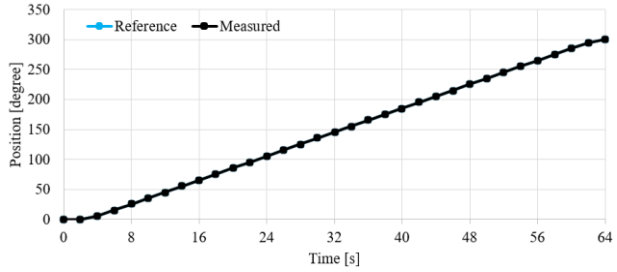

Fig. 12 The step-response of the control system.

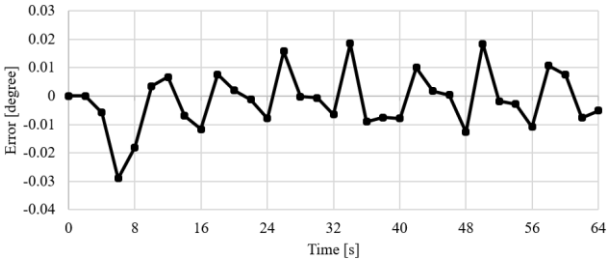

Fig. 13 The error between reference and motor position for a ramp reference input.

References

[1] S. Morimoto, M. Sanada, and Y. Takeda, "High-performance current-sensorless drive for PMSM and SynRM with only low-resolution position sensor," *IEEE Transactions on Industry Applications*, Vol. 39, No. 3, pp. 792–801, May 2003.

[2] J. Lemmens, P. Vanassche, and J. Driesen, "PMSM drive current and voltage limiting as a constraint optimal control problem," *IEEE Journal of Emerging and Selected Topics in Power Electronics*, Vol. 3, No. 2, pp. 326–338, Jun. 2015.

[3] L. Xiaoquan, L. Heyun, and H. Junlin, "Load disturbance observer-based control method for sensorless PMSM drive," *IET Electric Power Applications*, Vol 10, No. 8, pp.735–743, Sep. 2016.

[4] Y. A. R. I. Mohamed, "A hybrid-type variable-structure instantaneous torque control with a robust adaptive torque observer for a high-performance direct-drive PMSM," *IEEE Transactions on Industrial Electronics*, Vol. 54, No. 5, pp. 2491–2499, Oct. 2007.

[5] Y. A. R. I. Mohamed, "A newly designed instantaneous-torque control of direct-drive PMSM servo actuator with improved torque estimation and control characteristics," *IEEE Transactions on Industrial Electronics*, Vol. 54, No. 5, pp. 2864–2873, Oct. 2007.

[6] S. Chi, Z. Zhang, and L. Xu, "Sliding-mode sensorless control of direct-drive PM synchronous motors for washing machine applications," *IEEE Transactions on Industry Applications*, Vol. 45, No. 2, pp. 582–590, Mar. 2009.

[7] G. S. Buja and M. P. Kazmierkowski, "Direct torque control of PWM inverter-fed AC motors-a survey," *IEEE Transactions on Industrial Electronics*, Vol. 51, No. 4, pp. 744–757, Aug. 2004.

[8] D. Casadei, F. Profumo, G. Serra, and A. Tani, "FOC and DTC: two viable schemes for induction motors torque control," *IEEE transactions on Power Electronics*, Vol. 17, No. 5, pp. 779–787, Sep. 2002.

[9] F. Korkmaz, İ. Topaloğlu, M. F. Çakir, and R. Gürbüz, "Comparative performance evaluation of FOC and DTC controlled PMSM drives," in *4th International Conference on Power Engineering, Energy and Electrical Drives*, Istanbul, Turkey, pp. 705–708, May 2013.

[10] M. Z. Bilgin and B. Çakir, "Neuro-PID position controller design for permanent magnet synchronous motor," in *International Conference on Natural Computation*, Springer, Berlin, Heidelberg, Germany, pp. 418–426, Sep. 2006.

[11] R. Kumar, R. A. Gupta, and B. Singh, "Intelligent tuned PID controllers for PMSM drive-A critical analysis," in *IEEE International Conference on Industrial Technology*, Mumbai, India, pp. 2055–2060, Dec. 2006.

[12] W. K. Wibowo and S. K. Jeong, "Genetic algorithm tuned PI controller on PMSM simplified vector control," *Journal of Central South University*, Vol. 20, No. 11, pp. 3042–3048, Nov. 2013.

[13] R. C. García, W. I. Suemitsu, and J. P. Pinto, "Precise position control of a PMSM based on new adaptive PID controllers," in *XI Brazilian Power Electronics Conference*, pp. 1081–1086, Sep. 2011.

[14] W. Jun and P. Hong, "A robust position controller design for PM synchronous motor using neural network," in *Control, Automation, Robotics and Vision Conference*, pp. 2134–2138, Dec. 2004.

[15] S. Brock, J. Deskur, and K. Zawirski, "Robust speed and position control of PMSM," in *ISIE'99. Proceedings of the IEEE International Symposium on Industrial Electronics (Cat. No. 99TH8465)*, Vol. 2, pp. 667–672, 1999.

[16] Y. Wang and J. Fei, "Adaptive fuzzy sliding mode control for PMSM position regulation system," *International Journal of Innovative Computing Information and Control*, Vol. 11, No. 3, pp. 881–891, Jun. 2015.

[17] M. N. Uddin, T. S. Radwan, M. A. Rahman, and G. H. George, "Fuzzy logic based position control of permanent magnet synchronous motor," in *Canadian Conference on Electrical and Computer Engineering*, Halifax, NS, pp. 93–97, 2000.

[18] Y. S. Kung and P. G. Huang, "High performance position controller for PMSM drives based on TMS320F2812 DSP," in *Proceedings of IEEE International Conference on Control Applications*, pp. 290–295, Sep. 2004.

[19] H. B. Shin and J. G. Park, "Anti-windup PID controller with integral state predictor for variable-speed motor drives," *IEEE Transactions on Industrial Electronics*, Vol. 59, No. 3, pp. 1509–1516, Mar. 2012.

[20] K. J. Åström and T. Hägglund, *PID controllers: Theory, design, and tuning*, Research Triangle Park, NC: Instrument Society of America, 1995.

[21] C. Bohn and D. P. Atherton, "An analysis package comparing PID anti-windup strategies," *IEEE Control Systems*, Vol. 15, No. 2, pp. 34–40, Apr. 1995.

[22] K. H. Ang, G. Chong, and Y. Li, "PID control system analysis, design, and technology," *IEEE Transactions on Control Systems Technology*, Vol. 13, No. 4, pp. 559–576, Jul. 2005.

[23] J. W. Jung, V. Q. Leu, T. D. Do, E. K. Kim, and H. H. Choi, "Adaptive PID speed control design for permanent magnet synchronous motor drives," *IEEE Transactions on Power Electronics*, Vol. 30, No. 2, pp. 900–908, Feb. 2015.

S. H. Montazeri was born in Yazd, Iran, on February 3, 1993. He received the B.Sc. degree from Yazd University, Yazd, Iran, in 2015 and the M.Sc. degree from Sharif University of Technology, Tehran, Iran, in 2017 both in Electrical Engineering. He is currently working toward the Ph.D. degree in Electrical Engineering at Amirkabir University of Technology, Tehran, Iran. His fields of interest are power electronic converters, application of power electronics in energy systems, and variable speed drives.

A. Damaki Aliabad was born in Yazd, Iran, on April 9, 1983. He received the B.Sc., M.Sc., and Ph.D. degrees in electrical engineering from Amirkabir University of Technology, Tehran, Iran, in 2005, 2007, and 2012, respectively. He is currently an Assistant Professor with the Electrical and Computer Engineering Faculty, Yazd University, Yazd, Iran. His main research interests include design, analysis, and manufacturing of electrical machines, drive and control of electrical motors, and also fault current limiters.

F. Zareh was born in Yazd, Iran, on August 21, 1992. He received the B.Sc., and M.Sc., and degrees in Electrical Engineering in 2014 and 2017 from Yazd University, Yazd, Iran. His research interests include drive and control of electrical machinery.

S. Aghaei received his M.Sc. (2007) and Ph.D. (2013) both in Electrical (Control) Engineering from Isfahan University of Technology, Isfahan, Iran. He is currently an Assistant Professor at the faculty of Electrical Engineering, Yazd University, Yazd, Iran. His main research interests include distributed control of constrained systems, fault tolerant control of the constrained systems, control of time delay constrained systems, model predictive control, and reference governors. he also works on design and manufacturing innovative systems and has taken out some patents on his innovations. He was also selected as the premier researcher of Yazd province in the field of technology in 2019.